NANOSTRUCTURED ZINC OXIDE FOR WOUND DRESSINGS

Alexandra Elena STOICA (OPREA)[1], Alexandra Cătălina BÎRCĂ[2], Mihaela Loredana PIȚIGOI (PANDEL)[3], Alexandru Mihai GRUMEZESCU[4, 5, 6], Bogdan Ștefan VASILE[7,8], Florin IORDACHE[9], Anton FICAI[6, 10], Ecaterina ANDRONESCU[6, 11]

The present study reports the preparation and characterization of novel bioactive collagen wound dressing containing albumin and cinnamon essential oil functionalized ZnO nanoparticles. The purpose of this dressing was to enhance the efficacy of wound treatment. The wound dressings were physicochemical examined using Fourier-Transform infrared Spectroscopy (FTIR), Scanning Electron Microscopy (SEM), and Transmission Electron Microscopy (TEM). In vitro screening of dressings was performed using the MTT and GSH tests.

Keywords: dressing, zinc oxide, collagen, egg albumin, cinnamon oil.

[1] Ph.D. student., Dept. of Science and Engineering of Oxide Materials and Nanomaterials, National University of Science and Technology Politehnica Bucharest, Romania, e-mail: oprea.elena19@gmail.com

[2] Ph.D. student., Dept. of Science and Engineering of Oxide Materials and Nanomaterials, National University of Science and Technology Politehnica Bucharest, Romania, e-mail: ada_birca@yahoo.com

[3] Eng., Dept. of Science and Engineering of Oxide Materials and Nanomaterials, National University of Science and Technology Politehnica Bucharest, Romania, e-mail: loredana.pandel@yahoo.com

[4] Prof., Dept. of Science and Engineering of Oxide Materials and Nanomaterials, National University of Science and Technology Politehnica Bucharest, Romania, e-mail: grumezescu@yahoo.com

[5] CSI., ICUB—Research Institute of the University of Bucharest, Romania, e-mail: grumezescu@yahoo.com

[6] Prof., Academy of Romanian Scientists, Ilfov No. 3, 050044 Bucharest, Romania, e-mail: grumezescu@yahoo.com, anton.ficai@upb.ro, ecaterina.andronescu@upb.ro

[7] CS II., National Research Center for Micro and Nanomaterials, University Politehnica of Bucharest, Romania, e-mail: bogdan.vasile@upb.ro

[8] CS II., Research Center for Advanced Materials, Products and Processes, University Politehnica of Bucharest, Romania, e-mail: bogdan.vasile@upb.ro

[9] Lect., Department of Preclinical Sciences, Faculty of Veterinary Medicine, University of Agronomic Sciences and Veterinary Medicine of Bucharest, 105 Blvd. Splaiul Independentei, 050097 Bucharest, Romania, Romania, e-mail: floriniordache84@yahoo.com

[10] Prof., Dept. of Science and Engineering of Oxide Materials and Nanomaterials, National University of Science and Technology Politehnica Bucharest, Romania, e-mail: anton.ficai@upb. ro

[11] Prof., Dept. of Science and Engineering of Oxide Materials and Nanomaterials, National University of Science and Technology Politehnica Bucharest, Romania, e-mail: ecaterina.andronescu@upb.ro

1. Introduction

The process of wound healing is sometimes affected by infection resulting from the presence of monomicrobial or polymicrobial anaerobic and aerobic microorganisms that exhibit resistance to biocides and possess the capability to form dense biofilms. For several decades, researchers' primary objective in wound dressing has been to provide protection and coverage for wounds to prevent microbial infections [1]. Existing wound dressings exhibit several significant shortcomings, such as inadequate absorption of wound fluids, limited flexibility, a propensity to stick to the wound surface, insufficient mechanical strength, and an absence of an optimal moist environment conducive to wound healing. Furthermore, it is worth noting that a significant proportion of existing wound dressings lack antibacterial properties [2].

Collagen, constituting almost 30% of the total amount of protein mass, is the predominant extracellular matrix protein in animal species. The protein in discussion is classified as fibril, serving dual roles in structural support and functional processes. It actively participates in intricate systems related to tissue regulation, growth, and repair [3-5]. Due to collagen's decreased stability and weak mechanical strength, its potential use as a wound dressing material in clinical settings is severely limited [6]. Several studies have shown that the incorporation of nano-ZnO into collagen membranes results in increased mechanical strength and improved bioactivity [6-8].

Zinc is essential for the human body due to its intricate antibacterial mechanisms, which render it very effective against many antibiotic-resistant pathogens. Zinc oxide nanoparticles (ZnO NPs) exhibit bactericidal properties and are now utilized in a wide range of restorative products due to their notable characteristics, including a high surface area, a significant surface-to-volume ratio, a high catalytic efficiency and an excellent adsorption capacity [8,9]. Zinc oxide (ZnO) nanoparticles exhibit heightened antibacterial characteristics, demonstrating efficacy against medically significant microbial pathogens like *S. aureus* [10,11], *P. aeruginosa* [12-14], and *Escherichia coli* [1,15-18]. Despite an incomplete understanding of ZnO's mechanism of action, it has proven effective as an antibacterial agent in food packaging, tissue engineering and wound dressings [19].

Essential oils (EOs), also known as "volatile natural mixtures", represent secondary metabolites derived from plants that exhibit many beneficial properties such as anti-inflammatory, antioxidant, antiviral, antibacterial, anti-allergic and regenerative effects. Essential oils are primarily derived from various botanical components, including seeds, leaves, twigs, barks and roots of plants. One significant advantage is that essential oils exhibit minimal to no impact on the emergence and proliferation of antimicrobial resistance compared to antibiotics.

For instance, essential oils such as cinnamon, peppermint, lemongrass, lavender, tea tree, rosemary, thyme, and eucalyptus, among others, have been discovered to possess antibacterial characteristics [20-23].

The objective of this study is to integrate the regenerative characteristics of collagen with the antibacterial properties of egg albumin and zinc oxide nanoparticles (ZnO NPs) within the framework of developing and evaluating an enhanced collagen based wound dressing.

2. Experimental part

2.1. Materials

Zinc nitrate hexahydrate ($Zn(NO_3)_2 \cdot 6H_2O$), sodium hydroxide (NaOH) and methanol (CH_3OH) were acquired from Sigma-Aldrich (Merck Group, Darmstadt, Germany), collagen was obtained from the Leather And Footwear Research Institute (ICPI, Bucharest, Romania) and cinnamon oil (CO) was procured from Mayam. All of the reagents were of analytical-grade quality and did not require any additional purification before use.

2.2. Preparation of ZnO

The precipitation approach was used for the preparation of ZnO nanoparticles, and no additional thermal treatment was applied at any point in the process [24]. This method utilizing two different solutions. The first prepared solution consisted of a zinc precursor and was obtained by dissolving 3 g of $Zn(NO_3)_2 \cdot 6H_2O$ in 100 mL methanol (CH_3OH) under continuous stirring until a suitable level of homogenization. The another one, which served as the precipitation reagent, contained 3g NaOH solubilized in 100 mL of deionized water (DIW). A control sample of ZnO NPs was obtained by drop-wise addition of the alkaline precipitation reagent solution to the Zn precursor solution followed by vigorous stirring. Then, the initial clear solution gradually transforms, resulting in a milky white appearance. The nanoparticles were recuperated using centrifugation, and the white precipitate was then washed with DIW and dried in air.

2.3. Preparation of ZnO@CO

ZnO NPs surface-functionalized with cinnamon essential oil (CO) were obtained following the above-described method. The only difference is the addition of 500 µL of functionalizing agent (cinnamon essential oil) the precipitation alkaline reagent solution.

2.4. Preparation of ZnO, collagen, albumin, and cinnamon oil-based wound dressing

In order to obtain zinc oxide, collagen (CoL), egg albumin (EgA), and cinnamon oil (cO)-based wound dressing, a ZnO:CoL:EgA of 1:10:10 ratio was chosen. The concentration of utilized collagen was 2.3%. The EgA concentration was 55%. Thus, using the zinc oxide (ZnO) previously obtained, 6 samples were prepared:

Table 1

Samples prepared, and notation used

		Notation
Sample 1	Zinc oxide powder	ZnO
Sample 2	Zinx oxide powder functionalized with CO	ZnO@cO
Sample 3	ZnO:Collagen – 1:10	ZnO_CoL
Sample 4	ZnO: Collagen:Albumin – 1:10:10	ZnO_CoL_EgA
Sample 5	ZnO (with cO):Collagen – 1:10	ZnO@cO_CoL
Sample 6	ZnO (with cO):Collagen:Egg Albumin – 1:10:10	ZnO@cO_Col_EgA

Samples 3-6 were mechanically homogenized using a mechanical stirrer for 20 minutes at 800 rpm. Then, the samples were subjected to lyophilization. Thus, the samples are ready for physico-chemical and biological analyses.

2.5. Characterization methods

2.5.1. X-ray Diffraction (XRD)

Analysis of X-ray Diffraction were carried out with the assistance of a PANalytical Empyrean diffractometer (PANalytical, Almelo, The Netherlands), which was equipped with CuKα radiation a wavelength of 1.541874 Å, a hybrid 2 × Ge (220) monochromator for Cu, and a parallel plate collimator on the PIXcel3D detector. The experimental data were obtained within the range of 0-80° for the 2θ angles. The incidence angle was set at 0.5°, with a step size of 0.04° and a time step of 3 seconds. The data analysis was conducted utilizing the HighScore Plus program (version 3.0, PANalytical, Almelo, Netherlands).

2.5.2. **Fourier-Transform Infrared Spectroscopy (FTIR)**

IR spectra were collected by utilizing a Nicolet iN10 MX FT-IR microscope equipped with MCT (Hg–Cd–Te) liquid nitrogen cooled detector. The measurement range that was used was 400–4000 cm^{-1}. The spectral data was acquired using a reflection mode technique with a resolution of 8 cm^{-1}. In order to obtain each spectrum, a total number of 32 scans were combined and transformed into absorbance values using OmincPicta software, specifically the software provided by Thermo Scientific.

2.5.2. Scanning Electron Microscopy (SEM)

The study employed scanning electron microscopy (SEM) analysis, utilizing an FEI electron microscope. The examination involved using secondary electron beams with an energy level of 30 keV. The samples under investigation were coated with a thin layer of gold.

2.5.2. Transmission Electron Microscopy (SEM)

The ZnO nanopowders were observed using Transmission Electron Microscopy (TEM), and the images were captured on a Tecnai G2 F30 S-TWIN Transmission Electron Microscope with a resolution of 1 nm. This microscope is entirely analytical, and it is equipped with an EDX and STEM detector. The microscope had a working voltage of 300 kV during its operation.

2.5.3. In vitro tests

The assessment of cytotoxicity in the sample sections was conducted using the MTT test, specifically employing the Vybrant® MTT Cell Viability test Kit. The cells were grown on 96-well plates, with a seeding density of 3000 cells per well. Following incubation under various settings (24, 48, and 72 hours), a 10 µL volume of 12 mM MTT solution was introduced to the cultures, which were subsequently incubated at 37°C for an additional 4 hours. Following that, a volume of 100 µL of SDS-HCl solution was introduced, and the mixture was incubated for 1 hour. Subsequently, vigorous pipetting was performed to facilitate the solubilization of formazan crystals. The spectrophotometric measurement of absorbance at a wavelength of 570 nm was performed using the Infinite M200 equipment manufactured by TECAN (Männedorf, Switzerland).

Glutathione, often known as GSH, is a peptide composed of three amino acids found in eukaryotic organisms and functions as an antioxidant. Both oxidation and reactions with the thiol group, caused by reactive chemical species, can lead to a decrease in GSH levels. Changes in GSH levels are an essential part of the toxicological response assessment process. These changes can also induce oxidative stress, ultimately resulting in apoptosis and cell death. The GSH-GloTM Glutathione Assay is a luminescence-based assay that was developed by Promega in Madison, Wisconsin, United States. It was designed to detect and quantify levels of glutathione (GSH). The assay is based on the glutathione S-transferase (GST) process catalyzing the conversion of a luciferin derivative into luciferin in the presence of glutathione. In an associated reaction with firefly luciferase, the amount of glutathione present in the sample is directly proportional to the created signal. The protocol was performed according to the manufacturer's protocol. Briefly, we remove the culture medium from the adherent cells treated with and without zinc-based dressing and add 100µl of prepared 1X GSH Reagent to each well of a 96-well prepared in cell culture medium, mix briefly and incubate at

room temperature for 30 minutes. Next, was added 100 µl of reconstituted Luciferin Detection Reagent to each well of a 96-well plate, mixed briefly, incubated for 15 minutes, and measured the luminescence at a luminometer (TECAN, Männedorf, Switzerland).

3. Results and discussion

3.1. X-ray Diffraction (XRD)

The prepared ZnO and ZnO@cO NPs were characterized by X-ray Diffraction. The XRD spectra of ZnO appeared in the file of the standard International Center for Diffraction Data (ICCD). According to the ASTM Card with reference number 04-013-7122, the XRD planes of ZnO, which can be seen in Figures 1a and 1b, exhibit the characteristics of a single phase of the Wurtzite structure, which features hexagonal symmetry [25]. The XRD investigation of ZnO nanoparticles revealed diffraction peaks, which included (100), (002), (101), (102), (110), (103), (112), (201), (004) and (202) reflection planes of ZnO NPs having hexagonal phase. [26]. The peaks attributable to typical probable contaminants were not observed. The a high degree of crystallinityof ZnO can be deduced from the fact that the diffraction peaks are narrow.

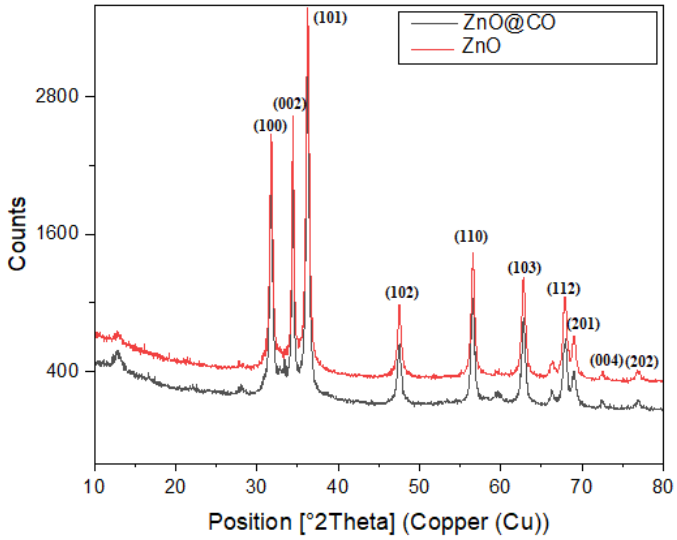

Fig. 1. The XRD pattern of ZnO and ZnO@cO.

3.2. Transmission Electron Microscopy (TEM)

In Fig. 4 is presented the obtained micrographs after TEM evaluation of the ZnO and ZnO@cO nanoparticles. This analysis highlights a quasi-spherical morphology of ZnO NPs (a1, a2) and also for ZnO@cO (b1, b2). At high

resolution, spherical ZnO was identified. This result agrees with XRD and SAED patterns (a3 and b3); the SAED images validating the Miller indices of specific crystalline structures.

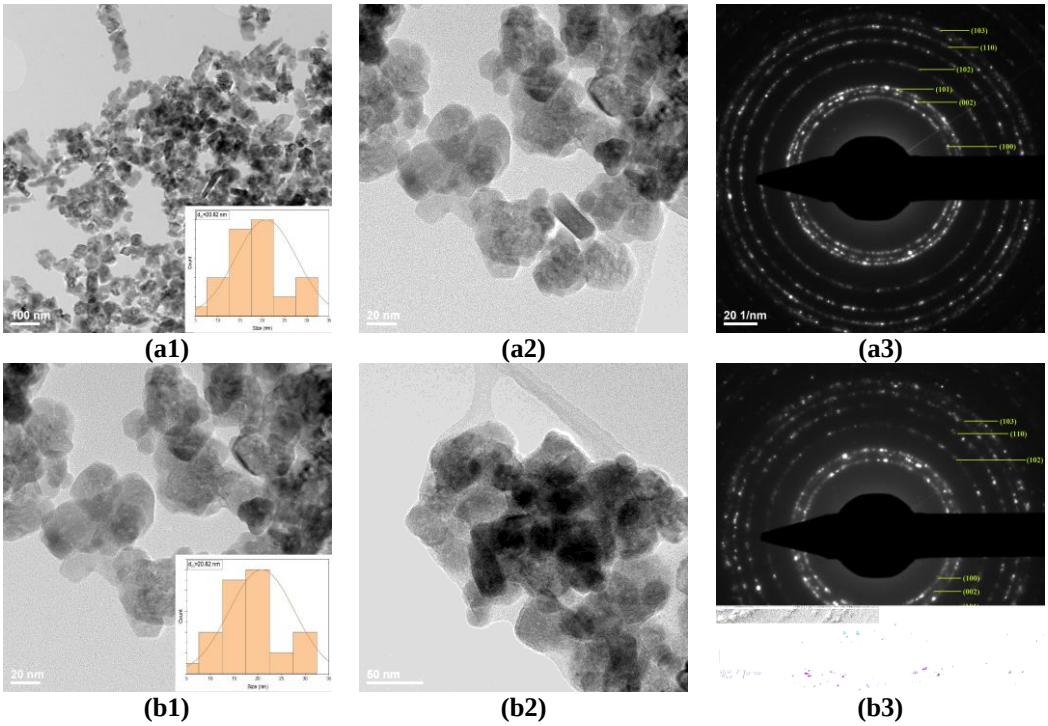

Fig 4. SEM images of (a1, a2, a3) ZnO and (b1, b2, b3) ZnO@cO.

3.3. Fourier-transform infrared spectroscopy (FTIR)

FTIR spectra of prepared samples are presented in Fig. 2. Zn–O bond was identified at ~527 cm^{-1}. The cinnamon essential oil extract (CO) shows absorption peaks between ~2900 cm^{-1} and ~2800 cm^{-1} that are characteristic to the C-H vibrations. .

The peak at ~3306 cm^{-1} is characteristic of amide groups, groups specific to the presence of collagen in the FTIR spectra. Type I amide groups correspond to the absorption spectrum located at 1628 cm^{-1}. Generally, the band with frequencies characteristic of type I amide groups, located in the range of 1600-1700 cm^{-1}, was mostly linked to the stretching vibrations of carbonyl groups [25].

The absorption bands between 1235 cm^{-1} and 1451 cm^{-1} provide information regarding the integrity of the triple helix collagen fiber. Amide groups of type II and III correspond to the absorption range located between the values of 1235 cm cm^{-1} and 1539 cm^{-1}, where N-H and C-H stretching vibrations can be identified. The band corresponding to the A-type amide group located at

3306 cm^{-1} corresponds to the N-H stretching vibrations and hydrogen bands present in collagen. The B-type amide group can be identified at 2935 cm^{-1} and was associated with the asymmetric stretches of the CH_2 group. In the FTIR spectrum, no major differences regarding the degradation of collagen functional groups during the synthesis process are identified. IR bands related to the albumin are masked by collagen bands.

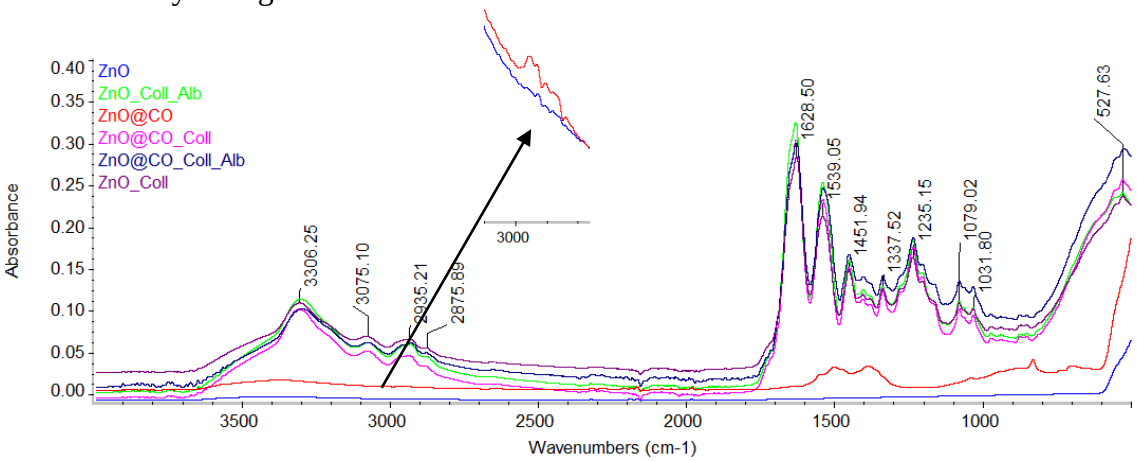

Fig. 2. FT-IR spectra of prepared samples.

3.4. Scanning Electron Microscopy (SEM)

Fig. 3 reveals the SEM images collected at different magnifications of the prepared samples.

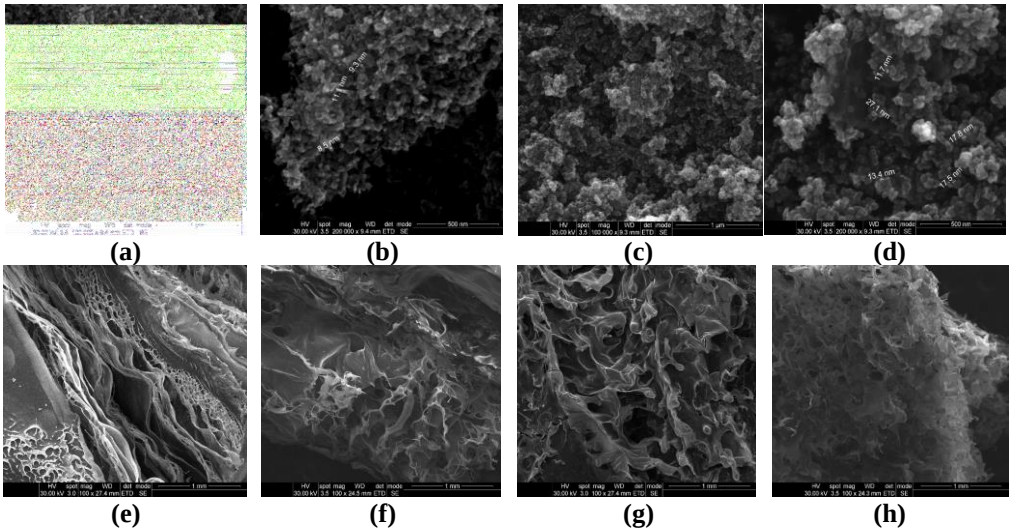

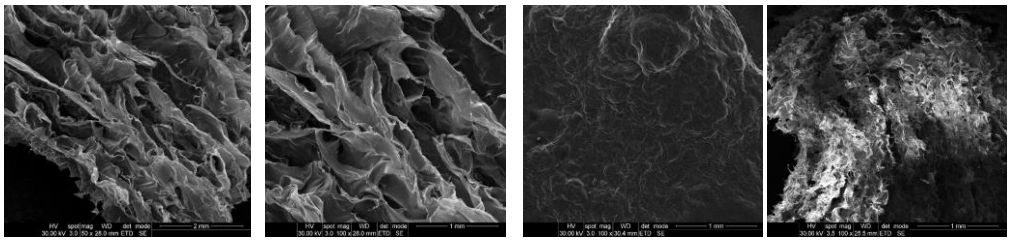

(i) **(j)** **(k)** **(l)**

Fig 3. SEM images of (a, b) ZnO, (c,d) ZnO@cO, (e, f) ZnO_CoL, (g, h) ZnO_CoL_EgA, (i, j) ZnO@cO_CoL, (k, l) ZnO@cO_CoL_EgA.

In the case of ZnO nanoparticles (a, b), it was determined an average diameter of around 10 nm. For ZnO@cO nanoparticles (c, d), it can be observed a predominantly spherical shape with a tendency of agglomeration of nanoparticles and dimensions ranging from 10 to 30 nm. Fig. 2 (e, f) also shows the scanning electron microscopy images for the sample containing ZnO_CoL, where it can be seen that the material obtained is very porous, with pores of different sizes. Both isolated and interconnected pores can be observed. In the case of ZnO@cO_CoL (i, j), the stratified and porous morphology is maintained. In the case of the ZnO_CoL_EgA and ZnO@cO_CoL_EgA samples (g, h, and k, l), it can be remarked a porous structure with fewer and smaller pores, unlike the sample without albumin. In this case, we can assume that the albumin modified the sample's morphology, making it denser.

3.5. In vitro tests

The oxidative stress of AFSC was determined by the level of glutathione produced by the ZnO@cO_CoL_EgA, ZnO@cO_CoL, ZnO_CoL, and ZnO_CoL_EgA samples, as shown in GSH Assay for AFSC after being in contact with the samples presented in Fig. 5. According to the findings, the materials did not cause an increase in the incidence of oxidative stress when they entered into contact with the AFSC. Oxidative stress occurs when the antioxidant defense system is unable to remove oxidants, resulting in a disruption of homeostasis [27]. The ZnO was found to have an effect on the equilibrium between antioxidant defense systems and oxidative stress [28].

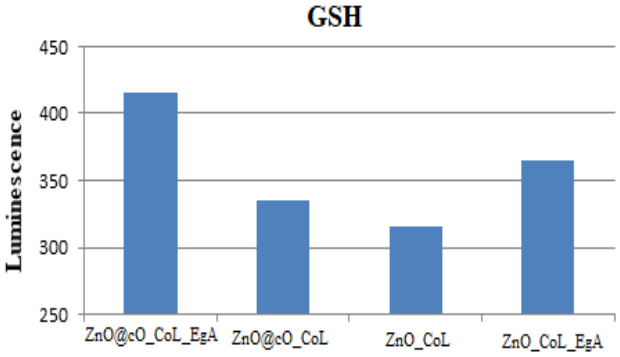

Fig. 5. GSH Assay for AFSC after being in contact with the samples.

The cytotoxicity of the dressings was evaluated using the MTT test. This assay provides data on cell viability following exposure to the samples at 24 hours, 48 hours, and 72 hours to zinc-based dressing materials. All samples exhibited favorable biocompatibility, with cell viability percentages consistently exceeding 80% across all three test time points. However, after 72 h, a non-important increase had be registered for ZnO_CoL, ZnO@cO_CoL, and ZnO_CoL_EgA samples, which implied that the materials did not have a proliferative effect on cells.

In the case of the ZnO@cO_CoL_EgA sample, after the first 48 h, it was observed an increase of almost 100% in cell viability compared to control. The biocompatibility of the ZnO@cO_CoL_EgA sample has been verified, indicating that mats is appropriate for use as a dressing that supports cell proliferation and growth. In tissue engineering and regenerative medicine, the use of zinc oxide (ZnO) nanoparticles in polymeric scaffolds has grown significantly. This is because they have valuable biological qualities like antibacterial properties, improved wound healing and cell proliferation [29,30]. Ullah et al. [29] reported the incorporation of ZnO NPs into chitosan-collagen 3D porous scaffolds. Their results showed that 3D porous scaffolds presented highest human fibroblasts cell proliferation [29]. Another type of 3D porous scaffolds based on chitosan/pectin/ZnO demonstrated biocompatibility, improved cell proliferation and migration [31].

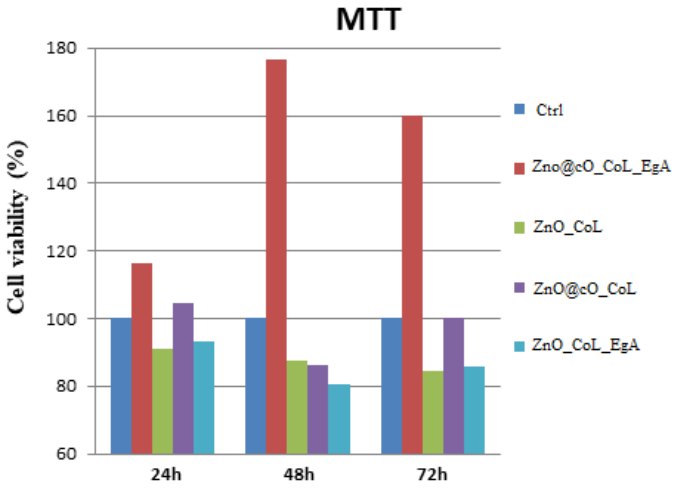

Fig. 6. Viability results of human endothelial cells cultured for 24 h, 48 h, and 72 h on prepared samples using the MTT assay (n = 3, * $p < 0.05$).

6. Conclusions

This study presents the synthesis and evaluation of wound dressings that incorporate collagen, egg albumin, and cinnamon essential oil functionalized ZnO nanoparticles. The materials obtained exhibit a stratified and porous structure, with isolated and interconnected pores. The porosity of wound dressings plays a crucial role in the healing process because it facilitates cell filtration, promotes high permeability, and enables the flow of oxygen and nutrients. The biocompatibility of the ZnO@cO_CoL_EgA sample was confirmed through an *in vitro* test, indicating that it can serve as a viable dressing material that promotes cell proliferation and growth. In this study, the MTT assay was employed to monitor cell viability and proliferation, while the GSH assay was utilized to assess the oxidative stress induced by the materials on AFSC. The choice of cinnamon essential oil turned out to be an inspired option. In this way, it is possible to demonstrate the suitability of such materials for wound dressing applications, which will provide biocompatibility.

Acknowledgment

This work was supported by the grant POCU/993/6/13-153178, co-financed by the European Social Fund within the Sectorial Operational Program Human Capital 2014–2020 and Romanian Governmental through the National Programme “Installations and Strategic Objectives of National Interest”.

REFERENCES

1. Rayyif, S.M.I.; Mohammed, H.B.; Curuțiu, C.; Bîrcă, A.C.; Grumezescu, A.M.; Vasile, B.Ș.; Dițu, L.M.; Lazăr, V.; Chifiriuc, M.C.; Mihăescu, G.; et al. ZnO Nanoparticles-Modified Dressings to Inhibit Wound Pathogens. Materials **2021**, 14, 3084.
2. Neacsu, I.-A.; Melente, A.E.; Holban, A.-M.; Ficai, A.; Ditu, L.-M.; Kamerzan, C.-M.; Tihăuan, B.M.; Nicoara, A.I.; Bezirtzoglou, E.; Chifiriuc, M.-C. Novel hydrogels based on collagen and ZnO nanoparticles with antibacterial activity for improved wound dressings. Romanian Biotechnological Letters **2019**, 24, 317-323.
3. Balaure, P.C.; Holban, A.M.; Grumezescu, A.M.; Mogoşanu, G.D.; Bălşeanu, T.A.; Stan, M.S.; Dinischiotu, A.; Volceanov, A.; Mogoantă, L. In vitro and in vivo studies of novel fabricated bioactive dressings based on collagen and zinc oxide 3D scaffolds. International Journal of Pharmaceutics **2019**, 557, 199-207, doi:https://doi.org/10.1016/j.ijpharm.2018.12.063.
4. Ricard-Blum, S. The collagen family. Cold Spring Harbor perspectives in biology **2011**, 3, a004978.
5. Lee, C.H.; Singla, A.; Lee, Y. Biomedical applications of collagen. International journal of pharmaceutics **2001**, 221, 1-22.
6. Chandraprabha, M.N.; Krishna, R.H.; Samrat, K.; Pradeepa, K.; Patil, N.C.; Sasikumar, M. Biogenic Collagen-Nano ZnO Composite Membrane as Potential Wound Dressing Material: Structural Characterization, Antibacterial Studies and In Vivo Wound Healing Studies. Journal of Inorganic and Organometallic Polymers and Materials **2022**, 32, 3429-3444, doi:10.1007/s10904-022-02351-8.
7. Vedhanayagam, M.; Unni Nair, B.; Sreeram, K.J. Collagen-ZnO Scaffolds for Wound Healing Applications: Role of Dendrimer Functionalization and Nanoparticle Morphology. ACS Applied Bio Materials **2018**, 1, 1942-1958, doi:10.1021/acsabm.8b00491.
8. Malathi, S.; Balashanmugam, P.; Devasena, T.; Kalkura, S.N. Enhanced antibacterial activity and wound healing by a novel collagen blended ZnO nanoparticles embedded niosome nanocomposites. Journal of Drug Delivery Science and Technology **2021**, 63, 102498, doi:https://doi.org/10.1016/j.jddst.2021.102498.
9. Stoica, A.E.; Chircov, C.; Grumezescu, A.M. Hydrogel Dressings for the Treatment of Burn Wounds: An Up-To-Date Overview. Materials **2020**, 13, 2853.
10. Ye, L.; He, X.; Obeng, E.; Wang, D.; Zheng, D.; Shen, T.; Shen, J.; Hu, R.; Deng, H. The CuO and AgO co-modified ZnO nanocomposites for promoting wound healing in Staphylococcus aureus infection. Materials Today Bio **2023**, 100552.
11. Banoee, M.; Seif, S.; Nazari, Z.E.; Jafari-Fesharaki, P.; Shahverdi, H.R.; Moballegh, A.; Moghaddam, K.M.; Shahverdi, A.R. ZnO nanoparticles enhanced antibacterial activity of ciprofloxacin against Staphylococcus aureus and Escherichia coli. Journal of Biomedical Materials Research Part B: Applied Biomaterials **2010**, 93, 557-561.
12. Ali, S.G.; Ansari, M.A.; Alzohairy, M.A.; Alomary, M.N.; Jalal, M.; AlYahya, S.; Asiri, S.M.M.; Khan, H.M. Effect of biosynthesized ZnO nanoparticles on multi-drug resistant Pseudomonas aeruginosa. Antibiotics **2020**, 9, 260.
13. Lee, J.-H.; Kim, Y.-G.; Cho, M.H.; Lee, J. ZnO nanoparticles inhibit Pseudomonas aeruginosa biofilm formation and virulence factor production. Microbiological research **2014**, 169, 888-896.

14. Bayroodi, E.; Jalal, R. Modulation of antibiotic resistance in Pseudomonas aeruginosa by ZnO nanoparticles. Iranian journal of microbiology **2016**, 8, 85.

15. Li, M.; Zhu, L.; Lin, D. Toxicity of ZnO nanoparticles to Escherichia coli: mechanism and the influence of medium components. Environmental science & technology **2011**, 45, 1977-1983.

16. Leung, Y.H.; Xu, X.; Ma, A.P.; Liu, F.; Ng, A.M.; Shen, Z.; Gethings, L.A.; Guo, M.Y.; Djurišić, A.B.; Lee, P.K. Toxicity of ZnO and TiO2 to Escherichia coli cells. Scientific reports **2016**, 6, 35243.

17. Zhang, L.; Jiang, Y.; Ding, Y.; Daskalakis, N.; Jeuken, L.; Povey, M.; O'neill, A.J.; York, D.W. Mechanistic investigation into antibacterial behaviour of suspensions of ZnO nanoparticles against E. coli. Journal of Nanoparticle Research **2010**, 12, 1625-1636.

18. Gudkov, S.V.; Burmistrov, D.E.; Serov, D.A.; Rebezov, M.B.; Semenova, A.A.; Lisitsyn, A.B. A mini review of antibacterial properties of ZnO nanoparticles. Frontiers in Physics **2021**, 9, 641481.

19. Tiplea, R.E.; Lemnaru, G.-M.; Trusca, R.; Holban, A.; Kaya, M.G.A.; Dragu, L.D.; Ficai, D.; Ficai, A.; Bleotu, C. Antimicrobial films based on chitosan, collagen, and zno for skin tissue regeneration. Biointerface Res. Appl. Chem **2021**, 11, 11985-11995.

20. Negut, I.; Grumezescu, V.; Grumezescu, A.M. Treatment Strategies for Infected Wounds. Molecules **2018**, 23, 2392.

21. Kalemba, D.; Kunicka, A. Antibacterial and antifungal properties of essential oils. Current medicinal chemistry **2003**, 10, 813-829.

22. Prabuseenivasan, S.; Jayakumar, M.; Ignacimuthu, S. In vitro antibacterial activity of some plant essential oils. BMC complementary and alternative medicine **2006**, 6, 1-8.

23. Deans, S.; Ritchie, G. Antibacterial properties of plant essential oils. International journal of food microbiology **1987**, 5, 165-180.

24. Spirescu, V.A.; Șuhan, R.; Niculescu, A.-G.; Grumezescu, V.; Negut, I.; Holban, A.M.; Oprea, O.-C.; Bîrcă, A.C.; Vasile, B.Ș.; Grumezescu, A.M.; et al. Biofilm-Resistant Nanocoatings Based on ZnO Nanoparticles and Linalool. Nanomaterials **2021**, 11, 2564.

25. Belabed, C.; Tab, A.; Bellal, B.; Belhamdi, B.; Benrakaa, N.; Trari, M. High photocatalytic performance for hydrogen production under visible light on the hetero-junction Pani-ZnO nanoparticles. International Journal of Hydrogen Energy **2021**, 46, 17106-17115, doi:https://doi.org/10.1016/j.ijhydene.2021.02.165.

26. Stan, M.S.; Constanda, S.; Grumezescu, V.; Andronescu, E.; Ene, A.M.; Holban, A.M.; Vasile, B.S.; Mogoantă, L.; Bălșeanu, T.-A.; Mogoșanu, G.D.; et al. Thin coatings based on ZnO@C18-usnic acid nanoparticles prepared by MAPLE inhibit the development of Salmonella enterica early biofilm growth. Applied Surface Science **2016**, 374, 318-325, doi:https://doi.org/10.1016/j.apsusc.2015.12.063.

27. Soneja, A.; Drews, M.; Malinski, T. Role of nitric oxide, nitroxidative and oxidative stress in wound healing. Pharmacological reports **2005**, 57, 108.

28. Hao, L.; Chen, L. Oxidative stress responses in different organs of carp (Cyprinus carpio) with exposure to ZnO nanoparticles. Ecotoxicology and Environmental Safety **2012**, 80, 103-110, doi:https://doi.org/10.1016/j.ecoenv.2012.02.017.

29. Ullah, S.; Zainol, I.; Idrus, R.H. Incorporation of zinc oxide nanoparticles into chitosan-collagen 3D porous scaffolds: Effect on morphology, mechanical properties and

cytocompatibility of 3D porous scaffolds. International Journal of Biological Macromolecules **2017**, 104, 1020-1029, doi:https://doi.org/10.1016/j.ijbiomac.2017.06.080.

30. Laurenti, M.; Cauda, V., ZnO nanostructures for tissue engineering applications. Nanomaterials **2017**, 7, 374.
31. Soubhagya, A.S.; Moorthi, A.; Prabaharan, M. Preparation and characterization of chitosan/pectin/ZnO porous films for wound healing. International Journal of Biological Macromolecules **2020**, 157, 135-145, doi:https://doi.org/10.1016/j.ijbiomac.2020.04.156.